

## Review

# Solid-State Nuclear Magnetic Resonance Spectroscopy: Theory and Pharmaceutical Applications

David E. Bugay<sup>1</sup>

---

The theory of solid-state nuclear magnetic resonance (NMR) spectroscopy is reviewed, with specific discussions of magnetic interactions in the solid state. Each magnetic interaction (Zeeman, dipole-dipole, chemical-shift, spin-spin, and quadrupolar) is addressed and manifestations of these interactions in the solid state NMR spectrum are explained. The techniques of high-power decoupling, magic-angle spinning, and cross-polarization, used to acquire highly resolved solid-state NMR spectra, are also illustrated. Application of solid-state NMR to pharmaceutical problem solving and methods development is then briefly reviewed.

**KEY WORDS:** solid-state nuclear magnetic resonance spectroscopy; cross-polarization/magic-angle spinning (CP/MAS); theory and pharmaceutical applications.

---

## INTRODUCTION

Nuclear magnetic resonance (NMR) spectroscopy in pharmaceutical research has been used primarily in a classical, organic chemistry framework. Typical studies have included (a) the structure elucidation of compounds, (b) investigating the chirality of drug substances, (c) the determination of cellular metabolism, and (d) protein studies, to name but a few. In each case, solution phase NMR has been utilized. Although ~90% of the pharmaceutical products on the market exist in the solid form, solid-state NMR is in its infancy as applied to pharmaceutical problem solving and methods development.

Drugs may exist in more than one polymorphic form (1). These forms sometimes display significant differences in solubility, bioavailability, processability, and physical/chemical stability (2). The study of the solid state of a pharmaceutical compound must take place not only at the bulk level, but also in the dosage form. Sometimes the extreme conditions of processing the formulation into the dosage form can alter the solid (3) or increase its interaction with excipients (4). Therefore, solid-state analytical techniques are important to characterize pharmaceutical solids.

With recent advances in NMR hardware and software development, the acquisition of high-resolution, multinuclear NMR spectra of pharmaceutical solids is now possible. Some of the advantages that exist for NMR in the solution phase exist in the solid state as well. Unfortunately, the same solution-phase disadvantages exist for solid-state NMR, in addition to the fact that magnetic interactions are of a much larger magnitude in the solid state than in the solution phase. However, these disadvantages may be overcome

by specific data acquisition techniques which yield highly resolved solid-state NMR spectra. Solid-state NMR is a non-destructive, multinuclear technique that has the ability to probe the chemical environment of each nucleus. Additionally, it is a quantitative technique that may be used in conjunction with other solid-state techniques such as thermal gravimetric analysis, microscopy, infrared spectroscopy, differential scanning calorimetry, and X-ray diffraction techniques (single crystal and powder) for the investigation of pharmaceutical solids.

This Review provides a basis of theory for solid-state NMR, in addition to a brief review of current pharmaceutical applications.

## SOLID-STATE NMR THEORY

Conventional utilization of solution-phase NMR data acquisition techniques on solid samples yields broad, featureless spectra (Fig. 1A). The broad nature of the signal is due primarily to dipolar interactions, which do not average out to zero in the solid state, and chemical shift anisotropy (CSA), which again is a function of the fact that our compound of interest is in the solid state. Before one describes the two principal reasons for the broad, featureless spectra, it is important to understand the main interactions that a nucleus with a magnetic moment experiences when situated within a magnetic field in the solid state. In addition, manifestations of these interactions in the solid-state NMR spectrum need to be discussed.

The principal interaction is the *Zeeman interaction* ( $H_Z$ ), which describes the interaction between the magnetic moment of the nucleus and the externally applied magnetic field,  $B_0$  (tesla). The nuclear magnetic moment,  $\mu$  (ampere meter<sup>2</sup>), is proportional to the nuclear spin quantum

$$\mu = \frac{\gamma h}{2\pi} \quad (1)$$

---

<sup>1</sup> Bristol-Myers Squibb Pharmaceutical Research Institute, 1 Squibb Drive, P.O. Box 191, New Brunswick, New Jersey 08903-0191.

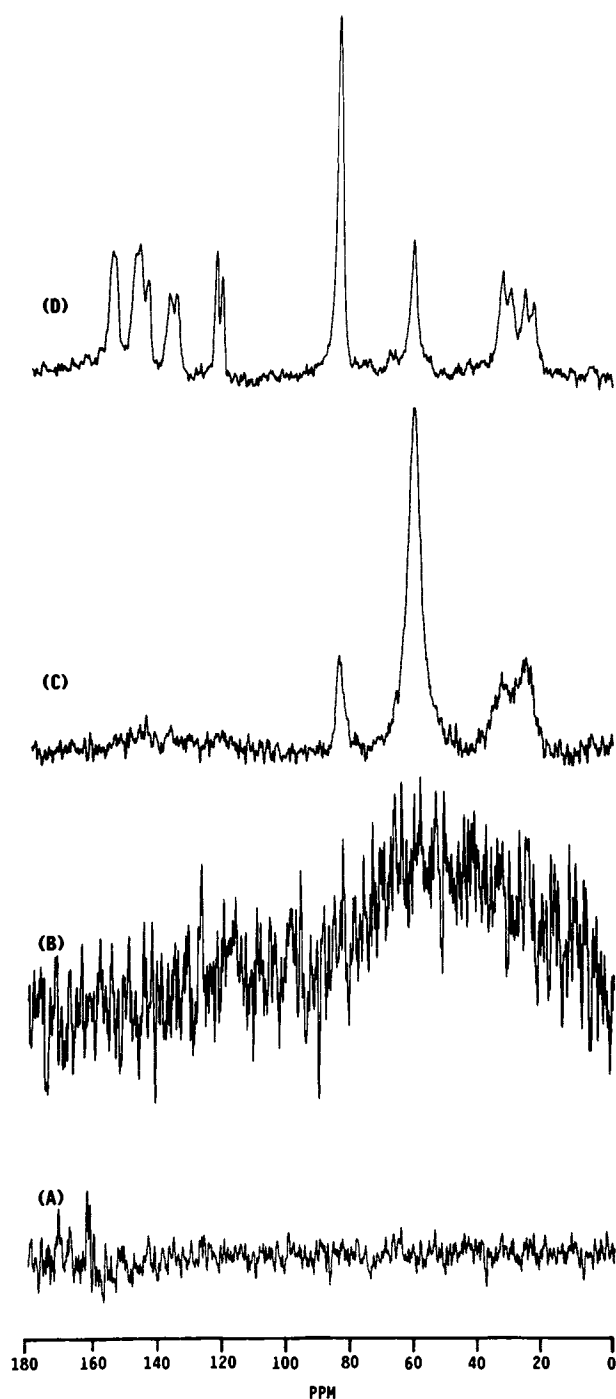


Fig. 1. Solid-state  $^{13}\text{C}$  NMR spectra of didanosine (VIDEX—ddI) acquired by (A) conventional solution-phase pulse techniques, (B) high-power proton decoupling only, (C) high-power proton decoupling and magic-angle spinning (5 kHz), and (D) high-power proton decoupling combined with magic-angle spinning (MAS) and cross-polarization (CP). In each case, 512 scans were accumulated.

number ( $I$ ) and the magnetogyric ratio ( $\gamma$ ; radian tesla $^{-1}$  second $^{-1}$ ), Eq. (1). Thus, the Zeeman interaction occurs only with nuclei which possess a spin greater than zero and yields  $2I + 1$  energy levels of separation  $\nu_0 = \gamma B_0/2\pi$ . Equation (2) describes the Hamiltonian where  $\nu_0$  is the corresponding Larmor frequency. The interaction is linear with

$$H_Z = -\gamma\hbar\vec{B}_0\vec{I}_Z \quad (2)$$

the applied magnetic field, thus giving the impetus to manufacture higher-magnetic field spectrometers, since a larger separation of energy levels leads to a greater population difference and a subsequent increase in the signal-to-noise ratio (S/N) within the measured spectrum. Since the Zeeman interaction incorporates the magnetogyric ratio, a constant for each particular nucleus, the resonant frequency for each nucleus is different at a specific applied magnetic field (Table I). The magnitude of the Zeeman interaction for a  $^{13}\text{C}$  nucleus in a 5.87-T magnetic field is 62.8 MHz. Small perturbations to the Zeeman effect are produced by other interactions such as dipole-dipole, quadrupolar, shielding, and spin-spin coupling. Typically, these small perturbations are less than 1% (<600 kHz) of the Zeeman interactions, which range in frequency from  $10^6$  to  $10^9$  Hz.

*Dipole-dipole interaction* is the direct magnetic coupling of two nuclei through space. This interaction may involve two nuclei of equivalent spin, or nonequivalent spin, and is dependent upon the internuclear distance and dipolar coupling tensor. Additionally, the total interaction, labeled  $H_D$ , is the summation of all possible pairwise interactions (homo- and heteronuclear). It is important to note that the interaction is dependent on the magnitude of the magnetic moments which is reflected in the magnetogyric ratio and on the angle ( $\theta$ ) that the internuclear vector makes with  $B_0$ . Therefore, this interaction is significant for spin  $1/2$  nuclei with large magnetic moments such as  $^1\text{H}$  and  $^{19}\text{F}$ . Also, the interaction decreases rapidly with increasing internuclear distance ( $r$ ), which generally corresponds to contributions only from directly bonded and nearest neighbor nuclei. Equation (3) describes the dipolar interaction for a pair of nonequivalent, isolated spins  $I$  and  $S$ . Since the dipolar cou-

$$H_D^{IS} = \frac{\gamma_I\gamma_S\hbar^2}{r^3}\vec{I}\cdot\vec{D}\cdot\vec{S} \quad (3)$$

pling tensor,  $D$ , contains a  $(1 - 3\cos^2\theta)$  term, this interaction is dependent on the orientation of the molecule. In solution-phase studies where the molecules are rapidly tumbling, the  $(1 - 3\cos^2\theta)$  term is integrated over all angles of  $\theta$  and subsequently disappears. Within solid-state NMR, the molecules are fixed with respect to  $B_0$ , thus the  $(1 - 3\cos^2\theta)$  term does not approach zero. This leads to broad resonances within the solid-state NMR spectrum since dipole-dipole interactions typically range from 0 to  $10^5$  Hz in magnitude.

In the case of pharmaceutical solids which are dominated by carbon and proton nuclei, the dipole-dipole interactions may be simplified. The carbon and proton nuclei may be perceived as "dilute" and "abundant" based upon their isotopic natural abundance, respectively (Table I). Homonuclear  $^{13}\text{C}$ - $^{13}\text{C}$  dipolar interactions essentially do not exist because of the low concentration of  $^{13}\text{C}$  nuclei (natural abundance of 1.1%). On the other hand,  $^1\text{H}$ - $^{13}\text{C}$  dipolar interactions contribute significantly to the broad resonances, but this heteronuclear interaction may be removed through simple high-power proton decoupling fields, similar to solution-phase techniques.

Table I. NMR Frequency Listing

Isotope	Spin	Natural abundance	Sensitivity		NMR frequency (MHz) at a field (T) of		
			Rel. <sup>a</sup>	Abs. <sup>b</sup>	2.35	5.87	11.74
1 H	1/2	99.98	1.00	1.00	100.00	250.00	500.00
2 H	1	1.5 × 10 <sup>-2</sup>	9.65 × 10 <sup>-3</sup>	1.45 × 10 <sup>-6</sup>	15.35	38.38	76.75
10 B	3	19.58	1.99 × 10 <sup>-2</sup>	3.90 × 10 <sup>-3</sup>	10.75	26.87	53.73
11 B	3/2	80.42	0.17	0.13	32.08	80.21	160.42
13 C	1/2	1.11	1.59 × 10 <sup>-2</sup>	1.76 × 10 <sup>-4</sup>	25.14	62.86	125.72
14 N	1	99.63	1.01 × 10 <sup>-3</sup>	1.01 × 10 <sup>-3</sup>	7.22	18.06	36.12
15 N	1/2	0.37	1.04 × 10 <sup>-3</sup>	3.85 × 10 <sup>-6</sup>	10.13	25.33	50.66
17 O	5/2	3.7 × 10 <sup>-2</sup>	2.91 × 10 <sup>-2</sup>	1.08 × 10 <sup>-5</sup>	13.56	33.89	67.78
19 F	1/2	100.00	0.83	0.83	94.08	235.19	470.39
23 Na	3/2	100.00	9.25 × 10 <sup>-2</sup>	9.25 × 10 <sup>-2</sup>	26.45	66.13	132.26
25 Mg	5/2	10.13	2.67 × 10 <sup>-3</sup>	2.71 × 10 <sup>-4</sup>	6.12	15.30	30.60
27 Al	5/2	100.00	0.21	0.21	26.06	65.14	130.29
29 Si	1/2	4.7	7.84 × 10 <sup>-3</sup>	3.69 × 10 <sup>-4</sup>	19.87	49.66	99.33
31 P	1/2	100.00	6.63 × 10 <sup>-2</sup>	6.63 × 10 <sup>-2</sup>	40.48	101.20	202.40
33 S	3/2	0.76	2.26 × 10 <sup>-3</sup>	1.72 × 10 <sup>-5</sup>	7.67	19.17	38.35
35 Cl	3/2	75.53	4.70 × 10 <sup>-3</sup>	3.55 × 10 <sup>-3</sup>	9.80	24.50	48.99
37 Cl	3/2	24.47	2.71 × 10 <sup>-3</sup>	6.63 × 10 <sup>-4</sup>	8.16	20.39	40.78
39 K	3/2	93.1	5.08 × 10 <sup>-4</sup>	4.73 × 10 <sup>-4</sup>	4.67	11.67	23.33
41 K	3/2	6.88	8.40 × 10 <sup>-5</sup>	5.78 × 10 <sup>-6</sup>	2.56	6.40	12.81
43 Ca	7/2	0.145	6.40 × 10 <sup>-3</sup>	9.28 × 10 <sup>-6</sup>	6.73	16.82	33.64
67 Zn	5/2	4.11	2.85 × 10 <sup>-3</sup>	1.17 × 10 <sup>-4</sup>	6.25	15.64	31.27
79 Br	3/2	50.54	7.86 × 10 <sup>-2</sup>	3.97 × 10 <sup>-2</sup>	25.05	62.63	125.27
81 Br	3/2	49.46	9.85 × 10 <sup>-2</sup>	4.87 × 10 <sup>-2</sup>	27.01	67.52	135.03
127 I	5/2	100.00	9.34 × 10 <sup>-2</sup>	9.34 × 10 <sup>-2</sup>	20.00	50.02	100.04
195 Pt	1/2	33.8	9.94 × 10 <sup>-3</sup>	3.36 × 10 <sup>-3</sup>	21.50	53.75	107.50

<sup>a</sup> Determined for an equal number of nuclei at a constant field.

<sup>b</sup> Product of the relative sensitivity and natural abundance.

The three-dimensional magnetic shielding by the surrounding electrons is an additional interaction that the nucleus experiences in either the solution or the solid state. This *chemical shift interaction* ( $H_{CS}$ ) is the most sensitive interaction to changes in the immediate environment of the nucleus and provides the most diagnostic information in a measured NMR spectrum. The effect originates from the small magnetic fields that are generated about the nucleus by currents induced in orbital electrons by the applied field. These small perturbations upon the nucleus are reflected in a change in the magnetic field experienced by the nucleus. Therefore, the field at the nucleus is not equal to the externally applied field and hence the difference is the nuclear shielding, or chemical shift interaction [Eq. (4)]. It is important to note the orientation dependence of the shielding constant,  $\sigma$ , and the fact that shielding is proportional to the

$$H_{CS} = \gamma_I \hbar \vec{I} \cdot \hat{\sigma} \cdot \vec{B}_0 \quad (4)$$

applied field, hence the need for chemical shift reference materials such as tetramethylsilane.

Solution-state NMR spectra yield "average" chemical shift values which are characteristic of the magnetic environment for a particular nucleus. The average signal is due to the isotropic motion of the molecules in solution. In other words,  $B_0$  "sees" an average orientation of a specific nucleus. For solid-state NMR, the chemical shift value is also characteristic of the magnetic environment of a nucleus, but normally, the molecules are not free to move. It must be kept in mind that the shielding will be characteristic of the nucleus

in a particular orientation of the molecule with respect to  $B_0$ . Therefore, a specific functional group oriented perpendicular to the magnetic field will give a sharp signal characteristic of this particular orientation (Fig. 2A). Analogously, if the functionality is orientated parallel to  $B_0$ , then a sharp signal characteristic of that orientation will be observed (Fig. 2B). For most polycrystalline pharmaceutical samples, a random distribution of all orientations of the molecule will exist. This distribution produces all possible orientations and is thus observed as a very broad NMR signal (Fig. 2C). The magnitude of the chemical shift anisotropy is typically between 0 and  $10^5$  Hz.

Two additional interactions experienced by the nucleus in the solid state are *spin-spin couplings* to other nuclei and *quadrupolar interactions*, which involve nuclei of spin greater than  $1/2$ . Spin-spin ( $H_{SC}$ ), or  $J$  coupling, originates from indirect coupling between two spins by means of their electronic surroundings and are several orders of magnitude smaller (possibly  $0-10^4$  Hz, typically only several kHz) than dipole interactions. Although  $J$  coupling interactions occur

$$H_{SC} = \vec{I} \cdot \vec{J} \cdot \vec{S} \quad (5)$$

in both the solid and the solution state, these couplings are typically used in solution-phase work for conformational analysis (5). Quadrupolar interactions ( $H_Q$ ) arise from dipolar coupling of quadrupolar nuclei, which display a non-

$$H_Q = \vec{I} \cdot \hat{Q} \cdot \vec{I} \quad (6)$$

spherically symmetrical field gradient, with nearby spin- $1/2$

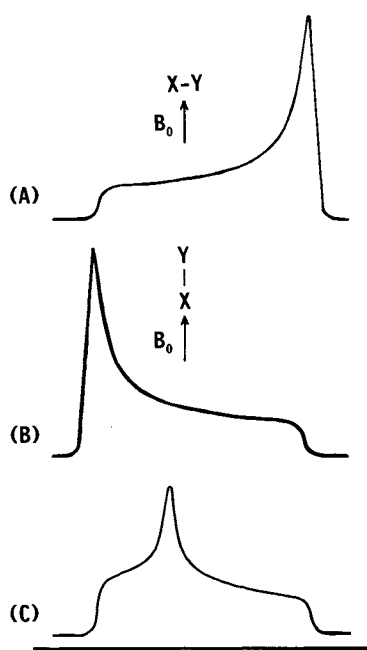


Fig. 2. Schematic representation of the  $^{13}\text{C}$  NMR signal of a single crystal containing the functional group A–B, oriented (A) perpendicular to the applied field and (B) parallel to the applied field. The lineshape in (C) represents the NMR signal of a polycrystalline sample with a random distribution of orientations yielding the chemical shift anisotropy pattern displayed.

nuclei. The magnitude of the interaction is dependent upon the relative magnitudes of the quadrupolar and Zeeman interactions and may completely dominate the spectrum (0–10<sup>9</sup> Hz), but since pharmaceutical compounds are primarily hydrocarbons, quadrupolar interactions typically do not interfere.

Summarizing the interactions, the isotropic motions of molecules in the solution state yield a discrete average value for the scalar spin–spin coupling and chemical shift interactions. For the dipolar and quadrupolar terms, the average obtained is zero, and the interaction is not observed in solution-phase studies. In sharp contrast, interactions in the solid state are orientation dependent, subsequently producing a more complicated spectrum, but one that contains much more information. In order to yield highly resolved, “solution-like” spectra of solids, a combination of three techniques is used: dipolar decoupling (6), magic-angle spinning (7,8), and cross-polarization (9). The remaining portion of this section discusses the three techniques and their subsequent effect upon measured spectra of pharmaceutical compounds which are dominated by carbon nuclei.

### Dipolar Decoupling

Discussed earlier was the fact that high-powered proton decoupling fields can eliminate the heteronuclear  $^1\text{H}$ – $^{13}\text{C}$  dipolar interactions that may dominate a solid-state NMR spectrum. The concept of decoupling is familiar to the solution-phase NMR spectroscopist but needs to be expanded for solid-state NMR studies. In solution-phase studies, the decoupling eliminates the scalar spin–spin coupling, not the dipole–dipole interactions (this averages out to zero due to

isotropic motions of the molecules). Irradiation of the sample at the resonant frequency of the nucleus to be decoupled ( $B_2$  field) causes the  $z$  component of the spins to flip rapidly compared to the interaction one wishes to eliminate. Scalar interactions usually require 10 W of decoupling power or less. In pharmaceutical solids work, decoupling is used primarily to remove the heteronuclear dipolar interactions between protons and carbons. The magnitude of the dipolar interaction (~50 kHz) usually requires decoupling fields of 100 W and subsequently removes both scalar and dipole interactions. Even with the use of high-power decoupling, broad resonances still remain, due principally to chemical shift anisotropy (Fig. 1B).

### Magic-Angle Spinning

Molecules in the solid state are in fixed orientations with respect to the magnetic field. This produces chemical shift anisotropic powder patterns for each carbon atom since all orientations are possible (Fig. 2). It was shown as early as 1958 that rapid sample rotation of solids narrowed dipolar-broadened signals (7). A number of years later, it was recognized that spinning could remove broadening caused by CSA yet retain the isotropic chemical shift (8).

The concept of magic-angle spinning arises from the understanding of the shielding constant,  $\sigma$  [Eq. (4)]. This constant is a tensor quantity and, thus, can be related to three principal axes where  $\sigma_i$  is the shielding at the nucleus when

$$\sigma_{ZZ} = \sum_{i=1}^3 \sigma_i \cos^2 \theta_i \quad (7)$$

$B_0$  aligns along the  $i$ th principal axis, and  $\theta_i$  is the angle this axis makes with  $B_0$ . Under conditions of mechanical spinning, this relationship becomes time dependent and a  $(3 \cos^2 \theta - 1)$  term arises. By spinning the sample at the so-called “magic angle” of 54.7°, or 54°44′, this term becomes zero and thus removes the spectral broadening due to CSA (Fig. 1C), providing that the sample rotation (kHz) is greater than the magnitude of the CSA (kHz).

CSA may range from 0 to 20 kHz so our spin rates must exceed this value or spinning side bands are observed. Figure 3A displays the solid-state  $^{31}\text{P}$  NMR spectrum of fosinopril sodium (Monopril), a novel ACE inhibitor (10), acquired under proton decoupling and static spinning conditions. At a relatively low spin rate of 2.5 kHz, broadening due to CSA is removed and the center band and side bands appear (Fig. 3B). As the sample is spun at higher rates (Figs. 3C and D), the side bands become less intense and move out from the center band. Even at a spin rate of 6 kHz (maximum spin rate for the probe/instrument used), the CSA is not completely removed (Fig. 3E). Although fast enough spin rates may not be achieved to remove CSA totally for specific compounds, slower than optimal rates will still narrow the resonances. Spinning side bands, at multiples of the spin rate, will complicate the spectrum, but they can be easily identified by varying the spin rate and observing which signals change in frequency. In addition, specific pulse sequences may be used to minimize the spinning side bands (11). While increasing the magnetic field strength increases the signal-

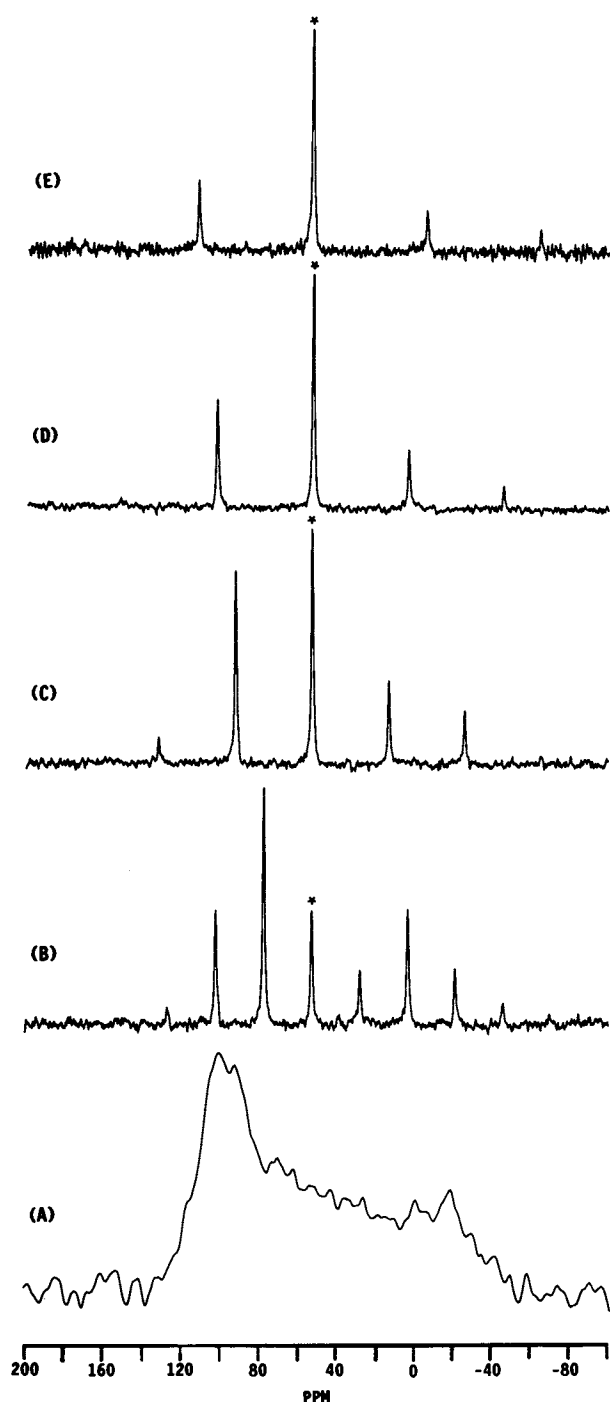


Fig. 3. Solid-state  $^{31}\text{P}$  NMR spectra of fosinopril sodium acquired under single-pulse, high-power proton decoupling and various conditions of magic-angle spinning: (A) static, (B) 2.5 kHz, (C) 4.0 kHz, (D) 5.0 kHz, and (E) 6.0 kHz. The isotropic chemical shift is designated by an asterisk.

to-noise ratio (Zeeman interaction), it also increases the CSA, since this interaction is field dependent [Eq. (4)]. Utilizing today's high-field spectrometers (>4.7 T), spinning side bands may exist but can be identified and used to gain additional information or be potentially eliminated if necessary.

The techniques of magic-angle spinning and heteronu-

clear dipolar decoupling produce solid-state NMR spectra which approach the linewidths and appearance of solution-phase NMR spectra. Unfortunately, there is an inherent lack of sensitivity in the general NMR experiment because of the nearly equivalent population of the two spin states for spin- $\frac{1}{2}$  nuclei. In addition, the sensitivity of the experiment is decreased with pharmaceutical compounds since they are composed primarily of carbon atoms where the  $^{13}\text{C}$  observable nuclei have a natural abundance of only 1%. The long relaxation times of specific carbon nuclei also pose a problem since quick, repetitive pulsing cannot occur. The technique of cross-polarization provides a means of both signal enhancement and reduction of long relaxation times.

#### Cross-Polarization

The concept of cross-polarization as applied to solid-state NMR was implemented by Pines *et al.* (9). A basic description of the technique is the enhancement of the magnetization of the rare spin system by transfer of magnetization from the abundant spin system. Typically, the rare spin system is classified as  $^{13}\text{C}$  nuclei and the abundant system as  $^1\text{H}$  spins. This is especially the case for pharmaceutical solids and the remaining discussion of cross-polarization focuses on these two spin systems only.

Figure 4 describes the cross-polarization (CP) pulse sequence and the behavior of the  $^1\text{H}$  and  $^{13}\text{C}$  spin magnetizations during the pulse sequence in terms of the rotating frame of reference (12). Step 1 of the sequence involves rotation of the proton magnetization onto the  $y'$  axis by application of a  $90^\circ$  pulse (rotating-frame magnetic field  $B_{1\text{H}}$ ). Subsequent spin-locking occurs along  $y'$  by an on-resonance pulse along  $y'$  for a specific period of time,  $t$ . At this point, a high degree of proton polarization occurs along  $B_{1\text{H}}$  which will decay with a specific time referred to as  $T_{1\rho\text{H}}$ . As the  $^1\text{H}$  spins are locked along  $y'$ , an on-resonance pulse,  $B_{1\text{C}}$ , is applied to the  $^{13}\text{C}$  spins. The  $^{13}\text{C}$  spins are also "locked" along  $y'$  and decay with the time  $T_{1\rho\text{C}}$ , (step 2). By correctly choosing the magnitude of the spin-locking fields  $B_{1\text{H}}$  and  $B_{1\text{C}}$ , the Hartmann-Hahn (13) condition [Eq. (8)] will be satisfied and transfer of magnetization will occur from the  $^1\text{H}$  spin reservoir to the  $^{13}\text{C}$  spin reservoir.

$$\gamma_{1\text{H}} B_{1\text{H}} = \gamma_{13\text{C}} B_{1\text{C}} \quad (8)$$

Once this equality is obtained by the correct spin-locking fields, the dilute  $^{13}\text{C}$  spins will take on the characteristics of the more favorable  $^1\text{H}$  system. In the end, a maximum magnetization enhancement equal to the ratio of the magnetogyric ratios may be achieved ( $\gamma_{\text{H}}/\gamma_{\text{C}}$ ). Once the carbon magnetization has built up during this "contact period" ( $t$ ),  $B_{1\text{C}}$  is switched off and the carbon free induction decay recorded (step 3). During this data acquisition period, the proton field is maintained for heteronuclear decoupling of the  $^1\text{H}$ - $^{13}\text{C}$  dipolar interactions. Step 4 involves a standard delay period in which no pulses occur and the two spin systems are allowed to relax back to their equilibrium states.

The entire CP pulse sequence provides two advantages for the solid-state NMR spectroscopist: significant enhancement of the rare spin magnetization and reduction of the delay time between successive pulse sequences since the rare spin system takes on the relaxation character of the

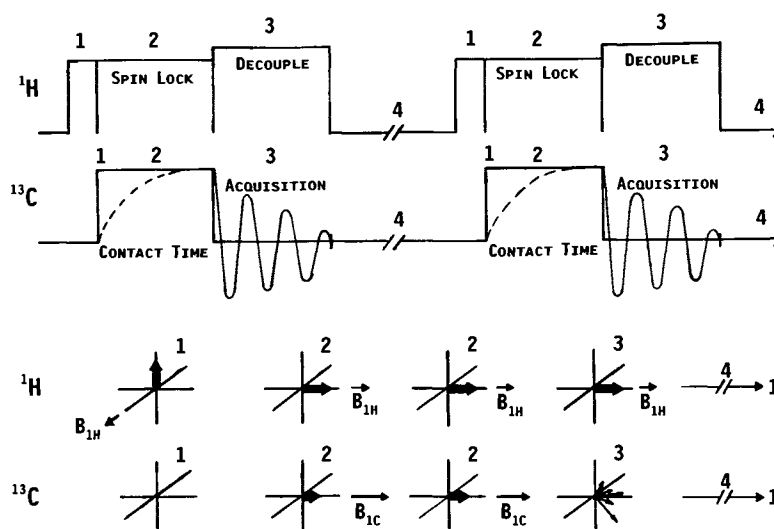


Fig. 4. The top diagram represents the pulse sequence for the cross-polarization experiment, whereas the bottom diagram describes the behavior of the  $^1\text{H}$  and  $^{13}\text{C}$  spin magnetizations during the sequence. The steps in the two diagrams correspond to each other and are fully explained in the text.

abundant spin system. Signal enhancement (magnetization enhancement) for less sensitive nuclei is immediately apparent from the CP process. Less obvious is the fact that the rare spin system signal is not dependent on the recycle time in step 4 (regrowth of carbon magnetization), but on the transfer process in step 2 and the relaxation behavior of the proton spin system in step 4. Since the single spin lattice relaxation time of the proton system is typically much shorter than the carbon system (1's to 10's versus 100's of seconds), the delay time is much shorter. This corresponds to a greater number of scans per unit time yielding better S/N.

Throughout the cross-polarization pulse sequence, a number of competing relaxation processes are occurring simultaneously. The recognition and understanding of these relaxation processes are critical in order to apply CP pulse sequences for quantitative solid-state NMR data acquisition or ascertaining molecular motions occurring in the solid state.

### Relaxation

Familiar to most chemists is the notion of spin-lattice relaxation (14). Labeled as  $T_1$ , the spin-lattice relaxation time is defined as the amount of time for the net magnetization ( $M_Z$ ) to return to its equilibrium state ( $M_0$ ) after a spin transition is induced by a radiofrequency pulse. The "lattice" term originates from the idea that the spin system gives up energy to its surroundings as it tries to reestablish spin

$$\frac{\partial M_Z}{\partial t} = \frac{-1}{T_1} (M_Z - M_0) \quad (9)$$

equilibrium. The process of transferring spin energy to other modes of energy may be classified as relaxation mechanism. For  $T_1$  in solids, all of the following mechanisms may con-

tribute: dipole-dipole ( $T_{1DD}$ ), spin rotation ( $T_{1SR}$ ), quadrupolar ( $T_{1Q}$ ), scalar ( $T_{1SC}$ ), and chemical shift anisotropy ( $T_{1CSA}$ ). The simple inversion-recovery pulse sequence may be used to measure  $T_1$  times for solid-state samples (15). In the use of simple high-powered decoupling, single-pulse sequences for quantitative NMR studies, the inversion-recovery pulse sequence may be used to determine  $T_1$ 's of interest. A multiple of five times  $T_1$  may then be incorporated as the recycle time between successive pulses assuring sufficient time for the magnetization to return to equilibrium. In this way, the NMR signal observed is truly representative of the number of nuclei producing it.

To understand the cross-polarization process, two other rate processes must be defined: (a) spin-lattice relaxation in the rotating frame ( $T_{1\rho}$ ) and (b) the cross-polarization relaxation time ( $T_{CH}$ ). The spin-lattice relaxation in a field  $B_1$  which is normally much smaller than the externally applied field  $B_0$ . In steps 1 and 2 of the CP sequence (Fig. 4), the carbon and proton spin systems are locked by the application of fields  $B_{1H}$  and  $B_{1C}$  and each system decays with its characteristic time. Figure 5 represents a thermodynamic model for the relaxation processes during CP. During contact between the two spin systems, magnetization is transferred at the rate  $T_{CH}$ . Since competing relaxation processes are occurring, the following conditions must be met to obtain a spectrum by CP:  $T_{1C} > T_{1H} \geq T_{1\rho H} > \text{CP time} > T_{CH}$ . It is apparent that for quantitative NMR studies of solids by CP, the individual relaxation processes must be measured to assure that the signal is truly proportional to the amount of species present.

With an understanding of magnetic interactions in the solid state, inherent relaxation processes, and experimental techniques to overcome these difficulties, Schaefer *et al.* acquired the first "liquid-like" NMR spectrum of a solid by CP/MAS techniques (16). Before a review of recent applications of CP/MAS NMR to the pharmaceutical sciences, the

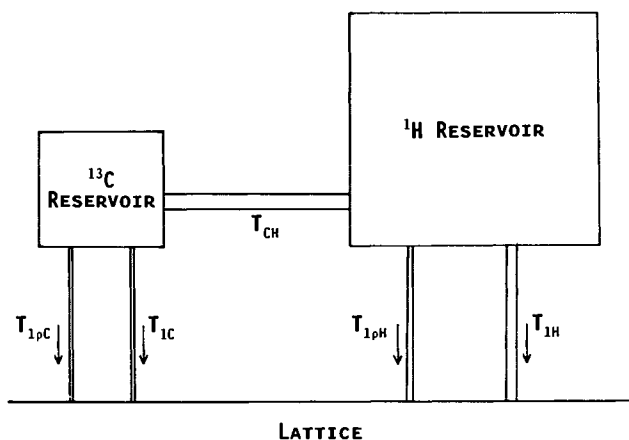


Fig. 5. Thermodynamic model of the cross-polarization sequence and representation of the competing relaxation processes.

brief Experimental section details some important information regarding practical solid-state NMR.

## EXPERIMENTAL

Manufacturers of today's modern NMR spectrometers normally offer a number of different models of instruments that are capable of measuring solid-state NMR spectra. Usually, a dedicated solid-state NMR instrument is available along with solution-phase models which are capable of solids work with the purchase of an additional solids accessory package. For any pharmaceutical company that is contemplating the purchase of an NMR for solids work, it is this author's opinion that a dedicated solid-state NMR instrument be purchased. Although this is not the venue to discuss the criteria for purchasing a solid-state NMR instrument, it is appropriate to comment briefly on instrumentation, types of samples that may be investigated, and a series of standard compounds that may be used for spectral referencing, MAS setting, and optimization of cross-polarization.

The basic components of the solid-state spectrometer are the same as the solution-phase instrument: data system, pulse programmer, observe and decoupler transmitters, magnetic system, and probes. In addition, high-power amplifiers are required for the two transmitters and a pneumatic spinning unit to achieve the necessary spin rates for MAS. Normally, the observe transmitter for  $^{13}\text{C}$  work requires broadband amplification of approximately 400 W of power for a 5.87-T, 250-MHz instrument. The amplifier should have

triggering capabilities so that only the radiofrequency (rf) pulse is amplified. This will minimize noise contributions to the measured spectrum. So that the Hartmann-Hahn condition may be achieved, the decoupler amplifier must produce an rf signal at one-fourth the power level of the observe channel for carbon work.

Any spectrometer system capable of doing complicated two-dimensional NMR work will have a sufficient data system and pulse programmer. The selection of the magnetic field strength is probably the hardest decision in the purchase process. Sensitivity and resolution improve with increasing field strength, yet spinning side bands are more prevalent. The intended use of the spectrometer system must be considered in the decision process for the correct magnetic field strength. The probes for solid-state NMR work are much different than their solution-phase counterparts. The typical solid-state NMR probe includes the standard irradiation and receiver electronics for the experiment, yet must include the hardware for magic-angle spinning. Normally, a double air bearing design is used for magic-angle spinning. This standard design permits high-speed spinning (3.5–5.0 kHz) with the ability for multinuclear data acquisition within a variable temperature range (normally 77–400 K). The rotors which contain the sample are constructed of zirconium oxide with either Kel-F caps for ambient temperature studies or boron nitride caps for variable temperature work. Depending upon the compressibility of the powdered, pharmaceutical sample, anywhere from 200 to 400 mg of sample is required to fill the rotor. In the Materials Science NMR laboratory at Bristol-Myers Squibb, a large number of nontraditional samples have been investigated by solid-state NMR (Table II). The main limitation is the ability to balance the rotor so that high-speed spinning may take place.

Although a series of standard referencing compounds has not been established for solid-state NMR, as opposed to solution-phase studies (17), a series of unofficial standard samples is currently being used (18). Table III lists a series of compounds, their intended use, and appropriate references further detailing their intended uses and limitations.

## APPLICATIONS

The most widely used application of solid-state NMR in the pharmaceutical industry is in the area of polymorphism, or pseudopolymorphism. The ability of a molecule to crystallize in more than one form is defined as polymorphism, whereas the ability to crystallize in more than one form based

Table II. Various Types of Pharmaceutical Samples Investigated by Solid-State NMR Spectroscopy

Sample	NMR nucleus	Brief description of studies
Bulk drug	$^{13}\text{C}$ , $^{31}\text{P}$ , $^{15}\text{N}$ , $^{25}\text{Mg}$ , $^{23}\text{Na}$	Solid-state structure elucidation, drug-excipient interaction studies (variable temperature), (pseudo-)polymorphic characterization at the qualitative and quantitative level, investigation of hydrogen bonding with salt compounds
Excipients	$^{13}\text{C}$ , $^{25}\text{Mg}$ , $^{23}\text{Na}$	Determination of the degree of cross-linking for polymer systems, drug-excipient interaction studies (variable temperature), (pseudo-)polymorphic characterization at the qualitative and quantitative level
Capsules	$^{13}\text{C}$ , $^{31}\text{P}$	Identifying residue from dissolution baths, drug-capsule interaction studies
Tablets	$^{13}\text{C}$ , $^{31}\text{P}$	Drug-excipient interaction studies, (pseudo-)polymorphic characterization at the qualitative and quantitative levels

Table III. Reference Samples for Solid-State NMR

Compound name	Intended use	Ref. no.
Adamantane (C <sub>10</sub> H <sub>16</sub> )	External referencing for <sup>13</sup> C spectra, optimizing Hartmann–Hahn match, linewidth measurement, sensitivity measurement	19
Hexamethylbenzene (C <sub>12</sub> H <sub>18</sub> )	Optimizing Hartmann–Hahn match	19
Glycine (C <sub>2</sub> H <sub>5</sub> O <sub>2</sub> N)	External referencing for <sup>13</sup> C spectra, sensitivity measurement, magic-angle setting for <sup>13</sup> C experimentation	19
Ammonium phosphate (NH <sub>4</sub> H <sub>2</sub> PO <sub>4</sub> ) monobasic	External referencing for <sup>31</sup> P spectra	19
Potassium bromide (KBr)	Magic-angle setting for <sup>13</sup> C experimentation	20
ZNP, <sup>a</sup> Zn[S <sub>2</sub> P(OC <sub>2</sub> H <sub>5</sub> ) <sub>2</sub> ] <sub>2</sub>	Magic-angle setting for <sup>31</sup> P experimentation	21
Samarium acetate tetrahydrate (CH <sub>3</sub> CO <sub>2</sub> ) <sub>3</sub> Sm · 4H <sub>2</sub> O	<sup>13</sup> C CP/MAS chemical-shift thermometer	22
TTAA <sup>b</sup>	<sup>15</sup> N CP/MAS chemical-shift thermometer	23

<sup>a</sup> Zinc(II) bis(*O,O'*-diethyldithiophosphate).

<sup>b</sup> 1,8-Dihydro-5,7,12,14-tetramethyldibenzo(b,i)-1,4,8,11-tetraazacyclotetradeca-4,6,11,13-tetraene-<sup>15</sup>N<sub>4</sub> [tetramethyldibenzotetraaza(14)annulene].

on the solvation state of the molecule is termed pseudopolymorphism. The use of solid-state NMR for the investigation of polymorphism is easily understood based on the following model. If a compound exists in two, true polymorphic forms labeled A and B, each crystalline form is conformationally different. This means, for instance, that a carbon nucleus in form A may be situated in a slightly different molecular geometry as compared to the same carbon nucleus in form B. Although the connectivity of the carbon nucleus is the same in each form, the local environment may be different. Since the local environment may be different, this leads to a different chemical shift interaction for each carbon and, ultimately, a different isotropic chemical shift for the same carbon atom in the two different polymorphic forms. If one is able to obtain pure material for the two forms, analysis and spectral assignment of the solid-state NMR spectra of the two forms can lead to the origin of the conformational differences in the two polymorphs. Solid-state NMR is thus an important tool in conjunction with thermal analysis, optical microscopy, IR spectroscopy, and powder and single-crystal X-ray crystallographic techniques for the study of polymorphism.

There are a number of significant advantages in the use of solid-state NMR for the study of polymorphism. As compared to diffuse reflectance IR and X-ray powder diffraction techniques, solid-state NMR is a bulk technique which does not have to consider particle size effects upon the intensity of the measured signal. In addition, NMR is an absolute technique under proper data acquisition procedures, meaning that the intensity of the signal is directly proportional to the number of nuclei producing it. By proper assignment of the NMR spectrum, the origin of the polymorphism can be inferred by differences in the resonance position for identical nuclei in each polymorphic form. Finally, the investigation of polymorphism by solid-state NMR can be performed at either the bulk drug or the dosage form level. This ability provides a significant tool for the investigation of polymorphic conversion under various processing techniques (e.g., various fluidized-bed granulation, dry blending, lyophilization, and tableting conditions).

The majority of applications of solid-state NMR used in

the investigation of pharmaceutical polymorphs is performed in conjunction with other analytical techniques. Byrn *et al.* have reported differences in the solid-state NMR spectra for different polymorphic forms of benoxaprofen and nabifone and pseudopolymorphic forms of cefazolin (24). Although single X-ray crystallography was initially used to study the polymorphs, the solid-state <sup>13</sup>C CP/MAS NMR spectrum of each form was distinctly different. These studies focused primarily on the bulk drug material, although a granulation of benoxaprofen was studied. It was concluded that solid-state NMR could be used to differentiate the form present in the granulation even in the presence of excipients. In further studies at Purdue University, the crystalline forms of prednisolone t-butylacetate (25), cefaclor dihydrate (26), and glyburide (27) were studied. The five crystal forms of prednisolone t-butylacetate were again determined by single X-ray crystallography and solid-state NMR used to determine the effect of crystal packing on the <sup>13</sup>C chemical shifts of the different steroid forms. Although conformational changes were observed in the ester side chain by X-ray crystallography, no major differences were noted in the NMR spectra, indicating that the environment remains relatively unchanged. Significant chemical shift differences were noted for carbonyl atoms involved in hydrogen bonding. This theme is consistent in the NMR study of cefaclor dihydrate. Again, the effects of hydrogen bonding were discernible by solid-state NMR. The study of glyburide was concerned principally with the structural conformation of the molecule in the solution and solid state. The solution conformation was determined by <sup>1</sup>H and <sup>13</sup>C NMR and in the solid by single-crystal X-ray crystallography, IR, and solid-state <sup>13</sup>C NMR. The solid-state NMR results suggested that this method would be useful for comparing solid- and solution-state conformations of molecules.

In a series of papers by Harris and Fletton, solid-state NMR has been used to investigate the structure of polymorphs. The majority of studies involves X-ray and IR techniques and also addresses the possibility of quantitative measurements of polymorphic mixtures. The three pseudopolymorphic forms of testosterone were examined by IR and <sup>13</sup>C CP/MAS NMR (28). The two forms of molecular spectros-



copy were able to differentiate the forms but NMR had the ability to investigate nonequivalent molecules in a given unit cell. A series of doublet resonances was noted for a series of different carbon atoms. This implied that the specific carbon atom within the molecule may resonate at two different frequencies depending on the crystallographic site of the molecule. In addition to the hydrogen-bonding explanation of the crystallographic splittings, the use of NMR to determine quantitatively the amount of each pseudopolymorph present in a mixture was addressed. In the study of androstanolone (29), high-quality  $^{13}\text{C}$  NMR spectra were obtained by CP/MAS techniques and allowed for characterization of the anhydrous and monohydrate forms. Again, crystallographic splittings were noted for the two forms and were related to hydrogen bonding. An identical approach to study pharmaceutical polymorphic structure was used in the investigation of the two polymorphs of 4'-methyl-2'-nitroacetanilide (30). An additional study of cortisone acetate (31) by solid-state NMR revealed differences in the NMR spectra for the six crystalline forms. Further multidisciplinary approaches to the physical characterization of pharmaceutical compounds are detailed in separate studies on cyclopenthiiazide (32), the excipient lactose (33), frusemide (34), and leukotriene antagonists MK-679, MK-571 (35), and L-660,711 (36). In each case solid-state NMR was used in conjunction with other techniques such as DSC, IR, X-ray diffraction, microscopy, and solubility/dissolution studies to characterize the polymorphic systems fully.

Additional studies of the solid-state structure of drug compounds by NMR in relation to X-ray crystallographic data include the compounds mofebutazone, phenylbutazone, oxyphenbutazone (37), and diphenhydramine hydrochloride (38). The topic of molecular recognition in which two molecules associate with specific intermolecular contacts (hydrogen bonding) has utilized NMR and X-ray techniques (39).

In further studies of polymorphism by solid-state NMR, conversion from one solid-state form to another by ultraviolet irradiation (40) and variable-temperature techniques (41) are outlined. In the first study, NMR was employed to follow the chemical transformation within the organic crystals of *p*-formyl-*trans*-cinnamic acid (*p*-FCA). A photoreactive  $\beta$ -phase may be crystallized from ethanol, whereas a photostable  $\gamma$ -phase is produced from acetone. After irradiation of the  $\beta$ -phase with UV radiation, and subsequent acquisition of the solid-state  $^{13}\text{C}$  NMR spectrum, the photoproduct was easily identified by NMR. The second conversion study (41) investigated the four forms of *p*-amino-benzenesulfonamide sulfanilamide ( $\alpha$ ,  $\beta$ ,  $\gamma$ , and  $\delta$ ). The first three forms were fully investigated by solid-state  $^{13}\text{C}$  NMR and X-ray crystallography techniques. Subsequent variable-temperature studies monitored the interconversion of the  $\alpha$  and  $\beta$  forms to the  $\gamma$  form. Coalescence of some NMR signals in the  $\gamma$  form also suggested that phenyl ring motion occurred within the crystal. Conclusions from the study indicated that solid-state NMR had the ability to differentiate pharmaceutical polymorphs, determine asymmetry in the unit cell, and investigate molecular motion within the solid state.

In a number of the publications describing the use of solid-state NMR for polymorphic characterization, the majority of the work has dealt with qualitative studies with brief

references to the possibility of quantitative analysis. An excellent guide to the utilization of magic-angle spinning and cross-polarization techniques for quantitative-solid state NMR data acquisition has been outlined by Harris (42). As mentioned before under Solid-State NMR Theory, in order to acquire solid-state NMR spectra in which the signal intensities truly reflect the nuclei producing them, data acquisition parameters such as recycle time, pulse widths, cross-polarization time, Hartmann-Hahn match, and decoupling power must be explicitly determined for each chemical system. In Harris's article, the problems of solid-state NMR acquisition techniques as applied to quantitative measurements are addressed. Additionally, errors in the setting of the magic angle, Hartmann-Hahn match, and cross-polarization mixing time are discussed in relation to obtaining quantitative NMR results.

Quantitative solid-state  $^{13}\text{C}$  CP/MAS NMR has been used to determine the relative amounts of carbamazepine anhydrate and carbamazepine dihydrate in mixtures (43). The  $^{13}\text{C}$  NMR spectra for the two forms did not appear different, although sufficient S/N for the spectrum of the anhydrous form required long accumulation times. This was determined to be due to the slow proton relaxation rate for this form. Utilizing the fact that different proton spin-lattice relaxation times exist for the two different pseudopolymorphic forms, a quantitative method was developed. The dihydrate form displayed a relatively short relaxation time permitting interpulse delay times of only 10 s to obtain full-intensity spectra of the dihydrate form while displaying no signal due to the anhydrous form. By utilizing an internal standard (glycine) and the differences in the relaxation rate of the two forms, the peak area of the dihydrate could be measured and related through a calibration curve to the amount of anhydrous and dihydrate content in mixtures of carbamazepine.

The conformational analysis of a number of pharmaceutical compounds has been studied by  $^{13}\text{C}$  NMR. The  $^{13}\text{C}$  CP/MAS NMR spectra of the three different forms of tartaric acid are reported in Ref. 44. The optically pure (+) form, the racemic form ( $\pm$ ), and the *meso*-tartaric acid form all displayed unique  $^{13}\text{C}$  NMR spectra. The possibility of the quantitative determination of optical purity and other physical properties determined by solid-state NMR is briefly discussed. A more complete study of conformational analysis by solid-state NMR is given by Díaz *et al.* for the compound methionine (45). Solid-state NMR results indicated that each crystalline form of DL-methionine consisted of a single conformer. Further NMR results, in conjunction with X-ray data, suggested that the L- or D-methionine crystal contains two different conformers in one unit cell.

Quantitative solid-state  $^{31}\text{P}$  NMR has been applied to the enantiomeric purity of organophosphorus compounds (46). The  $^{31}\text{P}$  MAS NMR spectra of *N*-[(diphosphono)methyl]-3-isobutylthiomorpholine displayed identical spectra for the (+) and (-) enantiomeric forms. The racemate, on the other hand, displayed a distinctly different spectrum as expected. Based upon the resonance positions and spinning side band intensity, the enantiomeric purity could be determined with an accuracy better than 1% by  $^{31}\text{P}$  MAS NMR. Similar results were also determined for a second organophosphorus compound.

Finally, a series of papers has been published on the

solid-state NMR spectra of a number of analgesic drugs. Jagannathan recorded the solid-state  $^{13}\text{C}$  NMR spectrum of acetaminophen in bulk and dosage forms (47). From the solution-phase NMR spectrum, assignments of the solid-state NMR resonances could be made in addition to explanations for the doublet structure of some resonances (dipolar coupling). Spectra of the dosage product from two sources indicated identical drug substances but different levels of excipients. The topic of drug-exci-pient interactions was addressed by solid-state  $^{13}\text{C}$  NMR in the investigation of different commercially available aspirin samples (48,49). In each commercial aspirin product, the only difference in the measured NMR spectrum was due to variations in the excipients, indicating that there were no interactions between the drug and the excipients under dry blending conditions. After lyophilization of two of the products, one aspirin sample did show a different NMR spectrum, indicating possible interaction during lyophilization or conversion to a different-solid state form during processing.

The multinuclear technique of solid-state NMR has been applied primarily to the study of polymorphism at the qualitative and quantitative levels. Although the technique ideally lends itself to the structure determination of drug compounds in the solid state, it is anticipated that in the future, solid-state NMR will be routinely used for method development and problem-solving activities in the analytical/materials science/physical pharmacy area of the pharmaceutical sciences.

## REFERENCES

1. A. Burger and R. Ramberger. On the polymorphism of pharmaceuticals and other molecular crystals. I. *Mikrochim. Acta (Wien)* II:259-271 (1979); A. Burger and R. Ramberger. On the polymorphism of pharmaceuticals and other molecular crystals. II. *Mikrochim. Acta (Wien)* II:273-316 (1979).
2. J. Haleblan and W. McCrone. Pharmaceutical applications of polymorphism. *J. Pharm. Sci.* 58:911-929 (1969).
3. M. Otsuka, T. Matsumoto, and N. Kaneniwa. Effects of the mechanical energy of multi-tableting compression on the polymorphic transformations of chlorpropamide. *J. Pharm. Pharmacol.* 41:665-669 (1989).
4. K. A. Connors, G. L. Amidon, and V. J. Stella. *Chemical Stability of Pharmaceuticals*, John Wiley & Sons, New York, 1986.
5. M. Karplus. Vicinal proton coupling in nuclear magnetic resonance. *J. Am. Chem. Soc.* 85:2870-2871 (1963).
6. T. C. Farrar and E. D. Becker. *Pulse and Fourier Transform NMR*, Academic Press, New York, 1971.
7. E. R. Andrew, A. Bradbury, and R. G. Eades. Removal of dipolar broadening of nuclear magnetic resonance spectra of solids by specimen rotation. *Nature* 183:1802-1803 (1959).
8. E. R. Andrew. The narrowing of NMR spectra of solids by high-speed specimen rotation and the resolution of chemical shift and spin multiplet structures for solids. *Prog. Nucl. Magnet. Reson. Spectrosc.* 8:1-39 (1972).
9. A. Pines, M. G. Gibby, and J. S. Waugh. Proton-enhanced nuclear induction spectroscopy. A method for high resolution NMR of dilute spins in solids. *J. Chem. Phys.* 56:1776-1777 (1972); A. Pines, M. G. Gibby, and J. S. Waugh. Proton-enhanced NMR of dilute spins in solids. *J. Chem. Phys.* 59:569-590 (1973).
10. A. Salvetti. Newer ACE inhibitors, a look at the future. *Drugs* 40:800-828 (1990).
11. W. T. Dixon, J. Schaefer, M. D. Sefcik, E. O. Stejskal, and R. A. McKay. Total suppression of sidebands in CPMAS carbon-13 NMR. *J. Magnet. Reson.* 49:341-345 (1982).
12. C. A. Fyfe. *Solid State NMR for Chemists*, CFC Press, Guelph, 1983.
13. S. R. Hartmann and E. L. Hahn. Nuclear double resonance in the rotating frame. *Phys. Rev.* 128:2042-2053 (1962).
14. R. J. Abraham, J. Fisher, and P. Loftus. *Introduction to NMR Spectroscopy*, John Wiley & Sons, New York, 1988, pp. 84-86.
15. T. C. Farrar and E. D. Becker. *Pulse and Fourier Transform NMR*, Academic Press, New York, 1971, pp. 20-22.
16. J. Schaefer, E. O. Stejskal, and R. Buchdahl. High-resolution carbon-13 nuclear magnetic resonance study of some solid, glassy polymers. *Macromolecules* 8:291-296 (1975).
17. P. Granger. Multinuclear NMR referencing. *Appl. Spectrosc.* 42:1-3 (1988).
18. W. L. Earl and D. L. VanderHart. Measurement of  $^{13}\text{C}$  chemical shifts in solids. *J. Magnet. Reson.* 48:35-54 (1982).
19. Bruker Instruments, Inc. *The CP/MAS Accessory Product Description Manual*, 1987.
20. J. S. Frye and G. E. Maciel. Setting the magic angle using a quadrupolar nuclide. *J. Magnet. Reson.* 48:125-131 (1982).
21. A. Kubo and C. A. McDowell. Setting of the magic angle for  $^{31}\text{P}$  MAS NMR using zinc(II) bis(O, $\text{O}'$ -diethylthiophosphate). *J. Magn. Reson.* 92:409-410 (1991).
22. G. C. Campbell, R. C. Crosby, and J. F. Haw.  $^{13}\text{C}$  chemical shifts which obey the Curie law in CP/MAS NMR spectra. The first CP/MAS NMR chemical-shift thermometer. *J. Magnet. Reson.* 69:191-195 (1986).
23. B. Wehrle, F. Aguilar-Parrilla, and H.-H. Limbach. A novel  $^{15}\text{N}$  chemical-shift NMR thermometer for magic angle spinning experiments. *J. Magnet. Reson.* 87:584-591 (1990).
24. S. R. Byrn, G. Gray, R. R. Pfeiffer, and J. Frye. Analysis of solid-state carbon-13 NMR spectra of polymorphs (benoxaprofen and nabilone) and pseudopolymorphs (cefazolin). *J. Pharm. Sci.* 74:565-588 (1985).
25. S. R. Byrn, P. A. Sutton, B. Tobias, J. Frye, and P. Main. The crystal structure, solid-state NMR spectra, and oxygen reactivity of five crystal forms of prednisolone tert-butylacetate. *J. Am. Chem. Soc.* 110:1609-1614 (1988).
26. H. Martinez, S. R. Byrn, and R. R. Pfeiffer. Solid-state chemistry and crystal structure of cefaclor dihydrate. *Pharm. Res.* 7:147-153 (1990).
27. S. R. Byrn, A. T. McKenzie, M. M. A. Hassan, and A. A. Al-Badr. Conformation of glyburide in the solid state and in solution. *J. Pharm. Sci.* 75:596-600 (1986).
28. R. A. Fletton, R. K. Harris, A. M. Kenwright, R. W. Lancaster, K. J. Packer, and N. Sheppard. A comparative spectroscopic investigation of three pseudopolymorphs of testosterone using solid-state IR and high-resolution solid-state NMR. *Spectrochim. Acta* 43A:1111-1120 (1987).
29. R. K. Harris, B. J. Say, R. R. Yeung, R. A. Fletton, and R. W. Lancaster. Cross-polarization/magic-angle spinning NMR studies of polymorphism: Androstanolone. *Spectrochim. Acta* 45A:465-469 (1989).
30. R. A. Fletton, R. W. Lancaster, R. K. Harris, A. M. Kenwright, K. J. Packer, D. N. Waters, and A. Yeadon. A comparative spectroscopic investigation of two polymorphs of 4'-methyl-2'-nitroacetanilide using solid-state infrared and high-resolution solid-state nuclear magnetic resonance spectroscopy. *J. Chem. Soc. Perkin Trans. II* 1705-1709 (1986).
31. R. K. Harris, A. M. Kenwright, B. J. Say, R. R. Yeung, R. A. Fletton, R. W. Lancaster, and G. L. Hardgrove, Jr. Cross-polarization/magic-angle spinning NMR studies of polymorphism: Cortisone acetate. *Spectrochim. Acta* 46A:927-935 (1990).
32. J. J. Gerber, J. G. vanderWatt, and A. P. Lötter. Physical characterization of solid forms of cyclopentiazide. *Int. J. Pharm.* 73:137-145 (1991).
33. H. G. Brittain, S. J. Bogdanowich, D. E. Bugay, J. DeVincendis, G. Lewen, and A. W. Newman. Physical characterization of pharmaceutical solids. *Pharm. Res.* 8:963-973 (1991).
34. C. Doherty and P. York. Frusemide crystal forms; Solid state and physicochemical analyses. *Int. J. Pharm.* 47:141-155 (1988).
35. R. G. Ball and M. W. Baum. A spectroscopic and crystallo-

- graphic investigation of the structure and hydrogen bonding properties of the chiral leukotriene antagonist MK-679 as compared to its racemate MK-571. *J. Org. Chem.* **57**:801–803 (1992).
36. E. B. Vadas, P. Toma, and G. Zografi. Solid-state phase transitions initiated by water vapor sorption of crystalline L-660, 711, a leukotriene D<sub>4</sub> receptor antagonist. *Pharm. Res.* **8**:148–155 (1991).
  37. M. Stoltz, D. W. Oliver, P. L. Wessels, and A. A. Chalmers. High-resolution solid-state carbon-13 nuclear magnetic resonance spectra of mofebutazone, phenylbutazone, and oxyphenbutazone in relation to x-ray crystallographic data. *J. Pharm. Sci.* **80**:357–362 (1991).
  38. R. Glaser and K. Maartmann-Moe. X-ray crystallography studies and CP-MAS <sup>13</sup>C NMR spectroscopy on the solid-state stereochemistry of diphenhydramine hydrochloride, an antihistaminic drug. *J. Chem. Soc. Perkin Trans.* **2**:1205–1210 (1990).
  39. M. C. Etter and G. M. Vojta. The use of solid-state NMR and x-ray crystallography as complementary tools for studying molecular recognition. *J. Mol. Graph.* **7**:3–11 (1989).
  40. K. D. M. Harris and J. M. Thomas. Probing polymorphism and reactivity in the organic solid state using <sup>13</sup>C NMR spectroscopy: Studies of *p*-formyl-*trans*-cinnamic acid. *J. Solid State Chem.* **93**:197–205 (1991).
  41. L. Frydman, A. C. Olivieri, L. E. Diaz, B. Frydman, A. Schmidt, and S. Vega. A <sup>13</sup>C solid-state NMR study of the structure and the dynamics of the polymorphs of sulphanilamide. *Mol. Phys.* **70**:563–579 (1990).
  42. R. K. Harris. Quantitative aspects of high-resolution solid-state nuclear magnetic resonance spectroscopy. *Analyst* **110**:649–655 (1985).
  43. R. Suryanarayanan and T. S. Wiedmann. Quantitation of the relative amounts of anhydrous carbamazepine (C<sub>15</sub>H<sub>12</sub>N<sub>2</sub>O) and carbamazepine dihydrate (C<sub>15</sub>H<sub>12</sub>N<sub>2</sub>O · 2H<sub>2</sub>O) in a mixture by solid-state nuclear magnetic resonance (NMR). *Pharm. Res.* **7**:184–187 (1990).
  44. H. D. W. Hill, A. P. Zens, and J. Jacobus. Solid-state NMR spectroscopy. Distinction of diastereomers and determination of optical purity. *J. Am. Chem. Soc.* **101**:7090–7091 (1979).
  45. L. E. Díaz, F. Morin, C. L. Mayne, D. M. Grant, and C. Chang. Conformational analysis of DL-, L-, and D-methionine by solid-state <sup>13</sup>C NMR spectroscopy. *Magnet. Reson. Chem.* **24**:167–170 (1986).
  46. K. V. Andersen, H. Bildsøe, and H. J. Jakobsen. Determination of enantiomeric purity from solid-state <sup>31</sup>P MAS NMR of organophosphorus compounds. *Magnet. Reson. Chem.* **28**:S47–S51 (1990).
  47. N. R. Jagannathan. High-resolution solid-state carbon-13 nuclear magnetic resonance study of acetaminophen: A common analgesic drug. *Curr. Sci.* **56**:827–830 (1987).
  48. C. Chang, L. E. Díaz, F. Morin, and D. M. Grant. Solid-state <sup>13</sup>C NMR study of drugs: Aspirin. *Magnet. Res. Chem.* **24**:768–771 (1986).
  49. L. E. Díaz, L. Frydman, A. C. Olivieri, and B. Frydman. Solid state NMR of drugs: Soluble aspirin. *Anal. Lett.* **20**:1657–1666 (1987).